J Braz. Soc. Mech. Sci. Eng. (2016) 38:1317–1324
DOI 10.1007/s40430-015-0429-y

TECHNICAL PAPER

Estimation of elastic moduli of particulate-reinforced composites using finite element and modified Halpin–Tsai models

I. Alfonso[1] · I. A. Figueroa[2] · V. Rodriguez-Iglesias[3] · C. Patiño-Carachure[3] · A. Medina-Flores[4] · L. Bejar[4] · L. Pérez[5]

Received: 29 May 2015 / Accepted: 5 September 2015 / Published online: 18 September 2015

Abstract In this paper, the effect of particle geometry on Young's modulus for particulate-reinforced composites was estimated using finite elements analysis (FEA) and modified Halpin–Tsai (HT) equations, including not only the effect of the aspect ratio but also the particle shape. This modified HT model includes a new parameter (a) which depends on the angle of the particle corners. FEA was used as a starting point to find the composites behavior depending on the reinforcement features, results that were compared to experimental values. Young's moduli and stresses distribution were estimated using an AlA356/SiC(p) composite as starting material . Selected particle geometries for modeling were cylinders, truncated cylinders, double cones, and double-truncated cones; while aspect ratios were modified from 0.6 to 1.8. There was an excellent agreement between experimental results, FEA, and modified Halpin–Tsai estimations, showing that the predicting ability of the Halpin–Tsai model could be improved by introducing different shape parameters.

Keywords Composite · FEA · Halpin–Tsai · Angle · Particles

Technical editor: Eduardo Alberto Fancello.

✉ I. Alfonso
ialfonso@unam.mx

[1] Unidad Morelia, Instituto de Investigaciones en Materiales, Universidad Nacional Autónoma de México, Campus Morelia UNAM, Antigua Carretera a Pátzcuaro No. 8701, Col. Ex-Hacienda de San José de la Huerta, C.P. 58190 Morelia, Michoacán, Mexico

[2] Instituto de Investigaciones en Materiales, Universidad Nacional Autónoma de México, Circuito Exterior SN. Ciudad Universitaria, Del. Coyoacán, C.P. 04510 Mexico, DF, Mexico

[3] Facultad de Ingeniería, Universidad Autónoma del Carmen, Campus III. Avenida Central S/N. Esq. con Fracc. Mundo Maya, Ciudad del, C.P. 24115 Carmen, Campeche, Mexico

[4] Universidad Michoacana de San Nicolás de Hidalgo, Ciudad Universitaria, C.P. 58000 Morelia, Michoacán, Mexico

[5] Department of Mechanical Engineering, Advanced Center for Electrical and Electronic Engineering (Basal Project FB0008), Universidad Técnica Federico Santa María, Av. España 1680, Casilla 110-V, Valparaiso, Chile

1 Introduction

Particle-reinforced metal matrix composites (MMCs) are materials that have been successfully used for many applications, mainly light MMCs, due to their attractive lightweight and superior mechanical and thermal properties [1–3]. Many of their properties are better than those of monolithic alloys tensile strength, elastic modulus, and high temperature stability; while other properties are considerably lower ductility, fatigue, and fracture toughness [4]. The properties of the MMCs depend on the reinforcement shape, volume fraction, distribution, aspect ratio, size, orientation, and interfacial bonding. There are numerous analytical and numerical models for the prediction of mechanical behavior of composite materials, with reasonably low errors, as the studied by Rafiee et al. [5] and Hashin et al. [6]. The analytical models mainly include the Eshelby model, the self-consistent model, the variational principles of elasticity theory, the composite cylinder model, and other unit-cell models. Numerical methods mainly include the finite difference method, the finite elements method (FEM or finite elements analysis, FEA), and the boundary element method [7, 8]. An easy way to evaluate the effective elastic response of a composite with perfect

particle–matrix bonding under load, is the conventional Rule of Mixtures. Nevertheless, this model does not take into account the particle aspect ratio, and is inexact when estimating the effective modulus of particulate MMCs. This approach is based on the condition of isostrain between the matrix and the reinforcement, and hence it is more exact for continuous fiber reinforcement with high aspect ratio. That is why other accurate estimations have been made in order to predict anisotropy in Young's modulus, e.g., the Halpin–Tsai (HT) model [9], which assumes a perfectly oriented discontinuous reinforcement in the composite, parallel to the applied load. According to the HT model, the Young's modulus can be determined by

$$E_c = \frac{E_m\left(1 + 2sqV_p\right)}{1 - qV_p}, \tag{1}$$

where E_c and E_m are, respectively, the Young's moduli of the composite and the matrix, s is the aspect ratio of the reinforcement, V_p its volume fraction, and q is a geometrical parameter that can be written as

$$q = \frac{\left(E_p/E_m\right) - 1}{\left(E_p/E_m\right) + 2s}, \tag{2}$$

where E_p the Young's modulus of the reinforcement.

HT model does not take into account all reinforcement features, although the shape fitting parameter (ξ) includes the aspect ratio (s), and in most cases $\xi = 2s$ [10]. That is why we think that experimental results and FEA estimations could be used combined to modified part of the HT model, including more particle features. FEA is a viable method to study particle-dispersed MMCs due to its modeling capability of the particle, being able to model different geometries, and analyze their effect on the composite properties, shown by Cook et al. [11]. Particles have been successfully modeled by Hanesh and Chawla [12] using 2D and 3D analysis with different reinforcement shapes cubic, cylinder, truncated cylinder, double cone, and sphere, obtaining different results. It is difficult to model the real microstructure of a composite due to the fact that particle distribution is likely to be random. That is why it is normally assumed that particles are arranged in a regular and periodic square, circular, or hexagonal array or unit cell. The selection of the unit cell is also critical for the estimations, where one particle or multi-particle models are normally used as representative volume element (RVE), as the works of Kari et al. [13]; Liu and Chen [14]; and Pahlavanpour et al. [15]. We have previously used FEA to analyze the case of the cylindrical model for particulate MMCs [16], comparing HT and FEA estimations. Nevertheless, it is important to study different particle models in order to obtain a better approach to the real MMC microstructure, and analyze the possibility to modify the HT model introducing a correction factor depending on the particle shape. HT model has been modified not only using s (aspect ratio) but also parameters that depend upon filler geometry, orientation, and loading direction, to fit the Halpin–Tsai equations to the experimental data [10, 17, 18]. Modifications also take into account the effect of interface, filler agglomerates, and anisotropy [19]. However, no works were found for predicting the effect of the reinforcement shape including a different particle feature (besides s). That is why the main objective of the present work is to analyze the possibility of including in the HT model the effect of another characteristic feature of the particles, specifically related to the particle corners. FEA was used to determine the effect of the particle geometry on tensile behavior, and for comparative purposes for modifying HT equations. Focusing to find the particle model that outputs the estimations in best concordance with experimental values, the models were obtained from experimental analyses of a MMC comprising SiC reinforcement particles into a Al–7.45Si–0.44Mg A356 alloy matrix.

2 Experimental and modeling

2.1 Composite microstructure

A MMC was obtained as 2 mm in diameter wires using the Ohno Continuous Casting (OCC) method [20], reinforcing an AlA356 alloy (Al–7.45Si–0.44Mg) with SiC particles. In order to determine the shape, volume fraction, average size, and aspect ratio of the reinforcement, the wires were polished using standard metallographic techniques and examined by optical microscopy. The obtained data, needed for modeling purposes, showed that the SiC particles presented irregular shapes, their minimum and maximum average lengths were 6.85 ± 1.75 and 14.02 ± 2.24 μm, respectively; while the volume fraction and average aspect ratio were 0.12 ± 0.02 and 1.40 ± 0.16, respectively. In order to establish the morphological characteristics of the MMC for the FEA models, experimentally observed irregular particles must be related to some standard geometric shape. Figure 1 shows an optical micrograph of the MMC obtained using the OCC process, remarking some geometric figures (from A to F) that could be used for modeling, in addition to other geometries not presented in this work.

The FEA model selected in this work for the MMC consisted of on assuming homogeneous distribution of the particles and a constant volume fraction of 0.12: particles with a volume of 610 μm^3 and the matrix with a volume of 5080 μm^3. Particle aspect ratios from 0.6 to 1.8 and different geometries were used, i.e., cylinder, double cone,

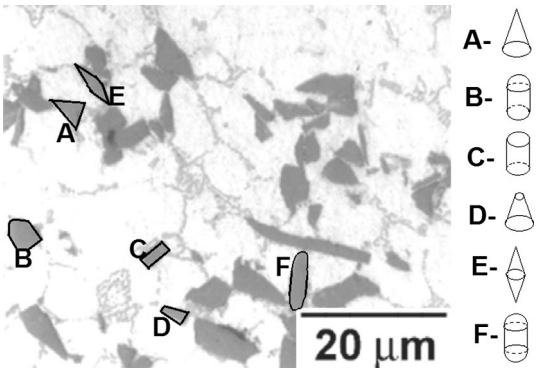

Fig. 1 Optical micrograph of the AlA356/SiC(p) MMC showing geometric figures that could correspond to the particle shapes: *A* cone, *B* partial rounded cylinder, *C* cylinder, *D* truncated cone, *E* double cone, and *F* rounded cylinder. Composite models

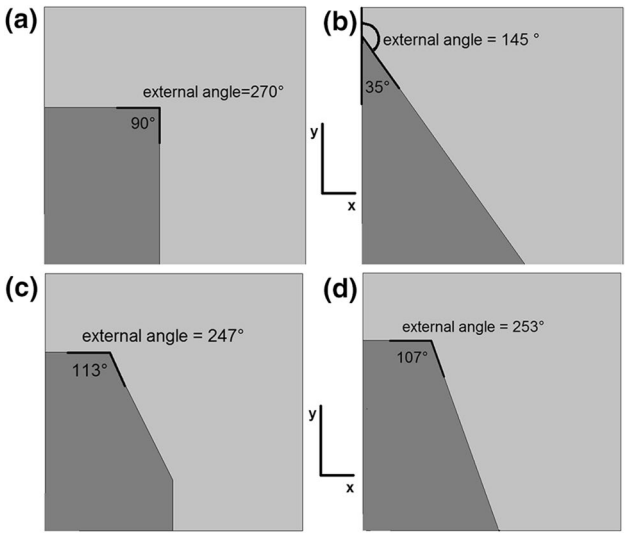

Fig. 2 Particle–matrix systems with different particle geometries and aspect ratios of 1.4 for: **a** cylinder, **b** double cone, **c** double-truncated cylinder, and **d** double-truncated cone

double-truncated cone, and double-truncated cylinder, as observed in Table 1. In the cases of double-truncated cone and truncated cylinder, for calculation purposes, the ratio between the radius of the base and the radius of the top was 2.0. Note that height and diameter values are dependent of the aspect ratio and the volume of the particles.

ANSYS 14.5 FEA software was employed for theoretical calculations. Cylindrical RVEs were obtained from the revolution of the square around *y* axis using the axi-symmetric capabilities of the ANSYS finite element code. Figure 2a–d shows planar RVEs for the models of particles with aspect ratios of 1.4 and different shapes, obtained from the analysis of Fig. 1. The angles of the corners are shown. As can be observed the external angles were also defined depending on the particle geometry. The obtained estimations will allow to determine the model that best represents the MMC.

The internal and external angles for the particle models observed in Fig. 2a–d are listed in Table 2 for different aspect ratios.

2.2 Simulation

An 8-Node 2D Structural Solid (Plane 82) triangular element was selected to create the finite element mesh. This element may be used as an axi-symmetric element. It is defined by eight nodes, having two degrees of freedom in each one, i.e., translations in the nodal *x* and *y* directions. Mesh convergence analysis was carried out by incrementally increasing the number of elements and verifying the local stress behavior, to ensure convergence of the numerical solution. The coupled-node boundary condition (keeping the nodes in the same plane) was used for *X* (upper) and *Y* (right) faces. This condition is applied, since the particles and the matrix have different moduli, provoking un-even surfaces, and making the deformation measurement hard to define [21]. Young's modulus can be obtained from the response of the tensile test, and along the *y* axis (E_y) can be determined by

$$E_y = \sigma_y/\varepsilon_y, \tag{3}$$

where σ_y and ε_y are the stress and the strain in *y* axis, respectively. The displacement of the RVE in *y* axis (u_y) is measured from the FEA estimations, and used for the strain determination

$$\varepsilon_y = u_y/\mathrm{L}_y, \tag{4}$$

where L_y is the original length of the RVE along *y* axis.

The properties of the materials used for the analyses are given in Table 3. The experimental Young's modulus for the

Table 1 Aspect ratios, diameters, and heights for different particle geometries

Aspect ratio (*h*/*d*)	Cylinder *h*/*d* (µm)	Double cone *h*/*d* (µm)	Truncated cone *h*/*d* (µm)	Truncated cylinder *h*/*d* (µm)
0.6	6.53/10.89	9.42/15.72	13.04/7.83	NP
1.0	9.19/9.19	13.26/13.26	11.00/11.00	11.00/11.00
1.4	11.5/8.21	16.58/11.84	13.77/9.83	12.94/9.24
1.8	13.59/7.55	NP	16.28/9.04	14.85/8.25

NP model is not possible

Table 2 Internal (i) and external (e) angles (in °) of the corners for different particle geometry models

Aspect ratio	Cylinder (*i*/*e*)	Cone (*i*/*e*)	Truncated cone (*i*/*e*)	Truncated cylinder (*i*/*e*)
0.6	90/270	57/123	130/230	NP
1.0	90/270	45/135	115/245	115/245
1.4	90/270	35/145	107/253	113/247
1.8	90/270	NP	104/256	113/247

NP model is not possible

Table 3 Mechanical properties for matrix and SiC particles [1, 22]

Material	Young's modulus, E (GPa)	Poisson ratio, ν
Al A356 Matrix	72.4	0.33
SiC particles	401.4	0.18

MMC was determined using a GrindoSonic Mk5, following ASTM E1876-97, and will be further compared to the estimated values.

Young's moduli of the MMCs with different particle geometries and aspect ratios were uni-axially estimated when applying a 5 MPa tensile stress on the upper end nodes of the RVE, and compared to both, HT model estimations using Eqs. (1) and (2), and experimental measurements. Different analyses of the effect of the angles of the particle corners on Young's modulus and stresses distribution were done to try to include a new shape parameter, and to obtain a modified HT model with improved predicting ability.

3 Results and discussion

Figure 3a shows the dependence, estimated using FEA, between the maximum axial stress and the aspect ratio for different particle geometries. As can be observed, maxima stresses slightly increase while the aspect ratio increases in similar ways for all modeled particle geometries, except for the double cone model, which abruptly increases and presents the highest stresses values. Models with the sharpest particles originate the highest degree of disturbance in the matrix and present the highest stresses values. After the analysis of these results, it was found that external angles can be used as a characteristic particle feature for relating the particle geometry to the composite behavior. Figure 3b shows the variation of the external angles depending on the aspect ratio for different particle models. This behavior for the external angles can be related to the maxima axial stresses behavior observed in Fig. 3a, increasing in similar way for each particle model, and being almost constant for cylinders. It is also important to notice that angle-maximum stress relation is inversely proportional; maxima stresses being for the the models with the lowest angles (cones), while the minima stresses were obtained for the models with the highest angles (cylinders).

As can be observed in Fig. 4, Young's modulus increases as the aspect ratio increases for all particle geometries, for estimations using both HT and FEA models. For low aspect ratios, the strengthening effect of the particles is low, increasing this effect for higher aspect ratios. Among the various theoretical methods to predict the elastic modulus

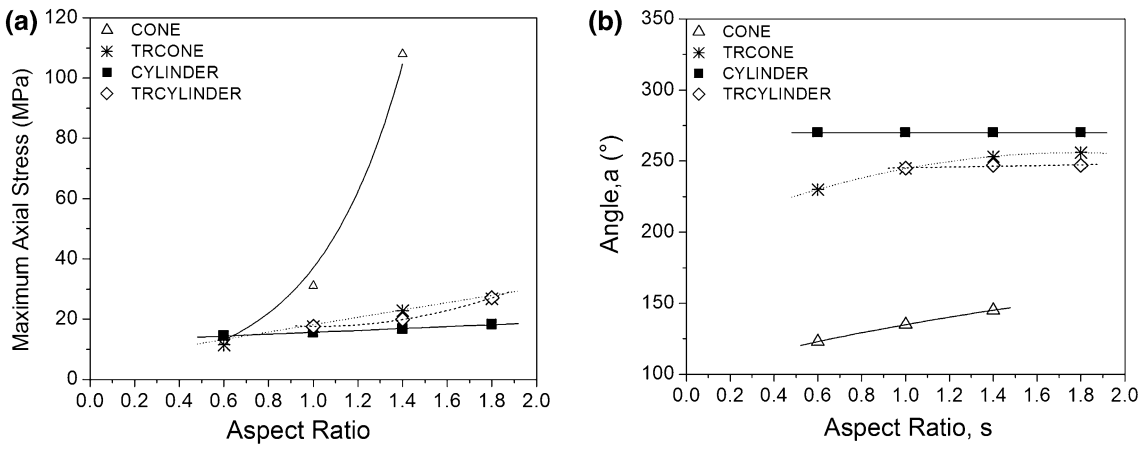

Fig. 3 **a** Maximum axial stress versus aspect ratio for the models under uni-axial load, and **b** external angles of the particle corners depending on the aspect ratio for different particle models

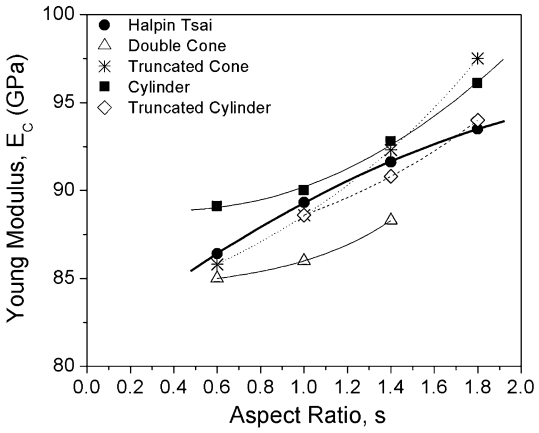

Fig. 4 Estimated Young's moduli versus particle aspect ratio for the MMCs using different models of particles

Table 4 Values of the angle factor (a) for different particle geometry models

Aspect ratio (h/d)	Cylinder	Cone	Truncated cone	Truncated cylinder
0.6	0.75	0.34	0.64	NP
1.0	0.75	0.38	0.68	0.68
1.4	0.75	0.40	0.70	0.69
1.8	0.75	NP	0.71	0.69

NP model is not possible

of the particulate dispersed MMCs, Halpin–Tsai equation is found to be closer to the experimental results. The advantage of FEA over these empirical equations is that it can model various types of particle shapes. That is why for HT model only one estimation can be obtained, as observed in Fig. 4. For FEA estimations, Young's moduli highest values were found for cylindrical particles and the lowest for double cones. Values in ascending order were for double cone, truncated cylinder, double-truncated cone, and cylinder, the same order that followed the external angles already observed in Fig. 3b. This fact remarks the important effect of the particle geometry on the composite behavior. The cylinder particle model presented the closest values to the experimental result (for an aspect ratio of 1.4 $E = 99.67 \pm 12.12$ GPa). These results show that the particles that preserve highest cross sections presented the highest Young's modulus. Cylindrical particles have a greater stiffening effect than rounded or sharp particles due to the fact that load is more effective across a planar interface [23]. It is important to notice that for particulate MMCs different particle geometries can be modeled, as was observed in Fig. 1, where the AlA356/SiC(p) MMC presented different particle shapes. The selection of the correct reinforcement geometry is very important in order to obtain a good correlation between simulated and experimental values. That is why it is important for an early analysis of the different particle features. Despite the variety of particle shapes that presented the MMC, the easiest one for modeling (cylinder) presented the best correlation with the experimental results, and the use of more complicated particle models would be unnecessary.

After the analysis of the above results, a modification to the HT equation is proposed, introducing an angle factor (a) that depends on the external angle of the corner of the particles (see Fig. 2a–d). This factor could be taken as a part of the already reported shape-fitting parameter ($\xi = 2s$) [10]. That is why the modified Halpin–Tsai equation could be re-written adding the factor a, as follows:

$$E_c = \frac{E_m\left(1 + 2saqV_p\right)}{1 - qV_p}, \tag{5}$$

where q can be calculated in its new form as

$$q = \frac{\left(E_p/E_m\right) - 1}{\left(E_p/E_m\right) + sa} \tag{6}$$

and as can be seen, $\xi = 2as$ instead of only $2s$.

For calculating the value of a, it is necessary to determine the external angle of the particles, as observed in Fig. 1, and then dividing this angle by 360°. For rounded particles the value of a is 1 ($a = 360°/360°$, no angles to measure, 360° is used), and the value of the Young modulus remains without any change. The values of a for different models are listed in Table 4.

Figure 5a–d shows the Young moduli estimations for different aspect ratios and particle shapes, using FEA, un-modified (Eqs. 1, 2) and modified (Eqs. 5, 6) Halpin–Tsai models. For all the particle models, the modified HT estimations are closer to the FEA predictions than for the un-modified HT model. This result is more remarkable for high aspect ratios and for the models of cylindrical (see Fig. 5a) and conical particles (see Fig. 5b). Comparing Young's moduli, the modified HT model presented the closest values (92.7 GPa, for cylinder) to the experimental results (99.67 ± 12.12 GPa, for particle aspect ratios of 1.4). The value for the un-modified HT model was 91.63 GPa. For the modified HT estimations, Young's modulus highest values were found for cylindrical particles, while the lowest were obtained for the double cone model. Values in ascending order were for double cone, truncated cylinder, double-truncate cone and cylinder.

Table 5 shows the differences (in %) between FEA and HT estimations, using modified and un-modified equations. As can be observed, the average difference is lower for modified HT equations than for un-modified. The most

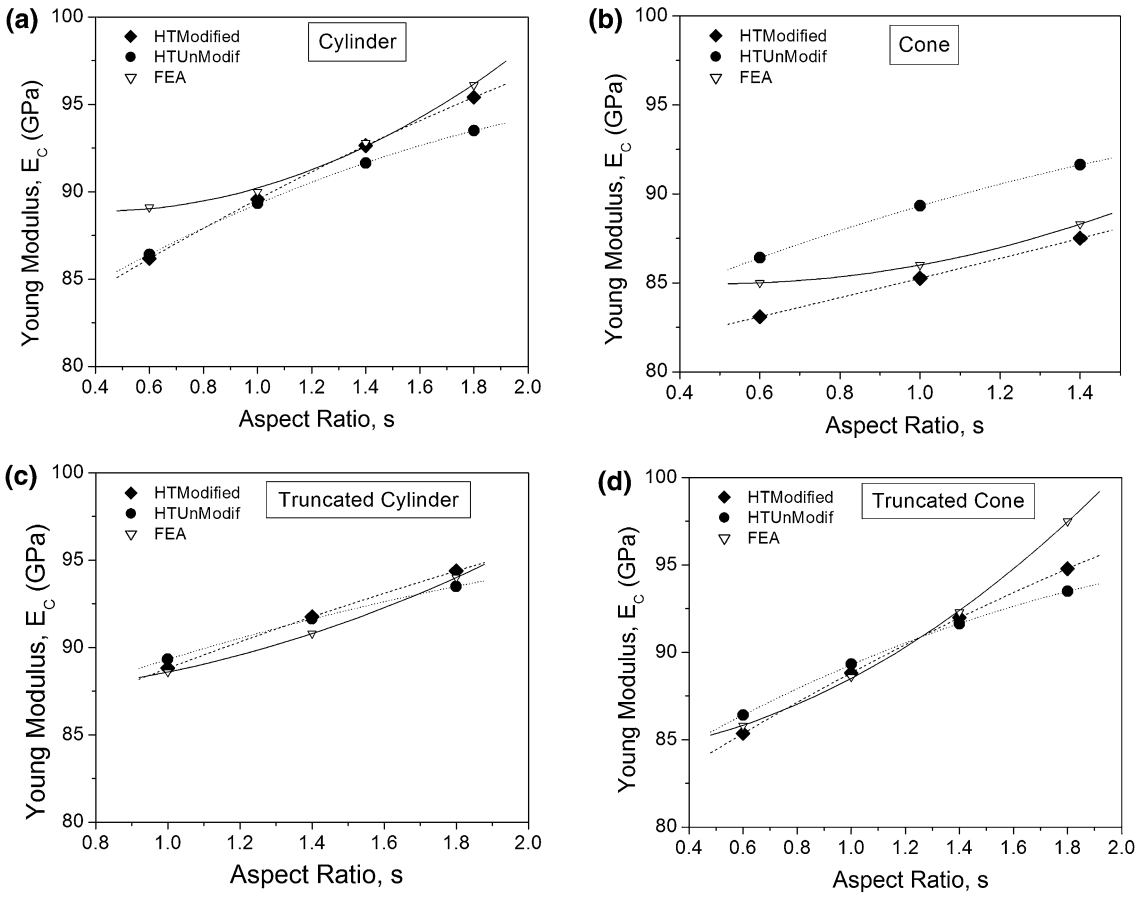

Fig. 5 Comparative estimated Young's moduli versus particle aspect ratio for the MMCs using FEA, un-modified, and modified HT models for different models of particle geometries: **a** cylinder, **b** double cone, **c** truncated cylinder, and **d** double-truncated cone

Table 5 Differences (in %) between FEA and HT estimations for modified and un-modified models

HT estimations (modified/un-modified)	Cylinder	Cone	Truncated cone	Truncated cylinder	Average
	1.17/1.94	1.34/3.09	0.97/1.59	0.56/0.75	1.01/1.84

significant differences were observed for cones, as also observed in Fig. 5b.

Results estimated using the modified HT model show that the predicting ability of the Halpin–Tsai model was improved by introducing the new parameter (a), being possible to estimate the Young's modulus for different particle geometries. Estimations obtained using this modification agree with different experimental and theoretical works, which state that composites with cylindrical reinforcements have higher Young's moduli than the composites reinforced with other kind of particles [23–25]. These works clearly show that particle shape has a significant influence on the overall tensile behavior of the composite. Cylindrical particles strengthen the composite more than the other shapes under a constant reinforcement fraction, and particles possessing the sharpest type of corners, as shown for double cone particles, presented the lowest strength. Truncated cylinders and spheres have similar behaviors [23]. Cylinder and double cone result in, respectively, the highest and the lowest degrees of disturbance of the local plastic flow paths in the matrix. This directly reflects the different extents of constrained plastic flow and hence the strengthening behavior in the composite. Figure 6a–d shows the stresses distribution for different particle geometries, and aspect ratios of 1.4. As can be observed, maxima stresses are located at the corners of the particle–matrix interfaces (see circles), exactly the points that were used for our modification to the HT model, demonstrating their importance. These results, beyond the possible error attributed to the RVE selection

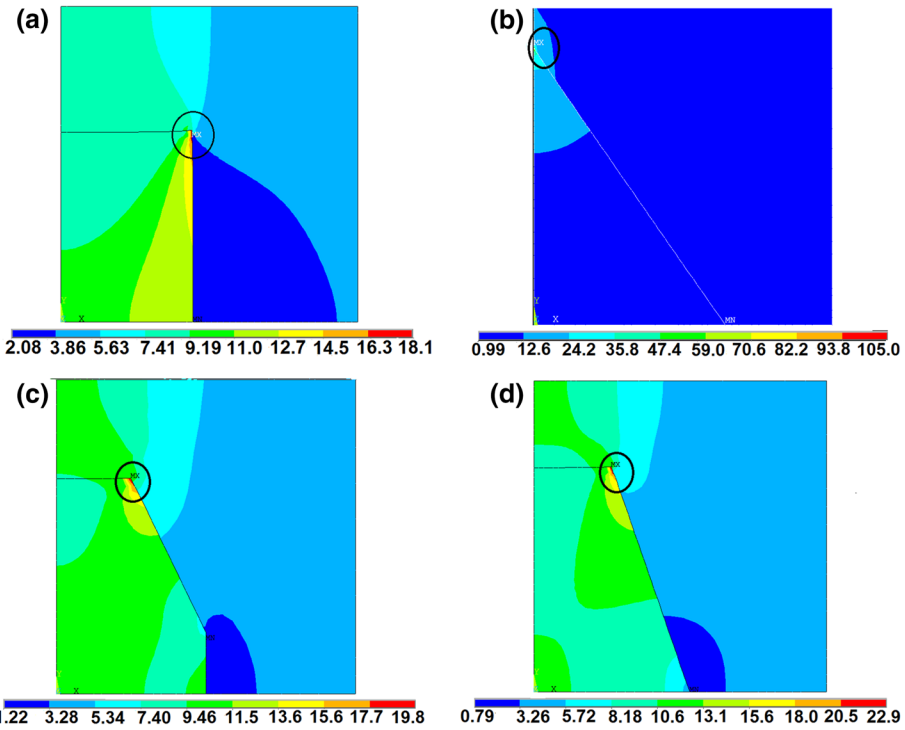

Fig. 6 Maxima axial stresses (in MPa) distribution for the models representing the MMC with particle aspect ratio of 1.4 and different geometries: **a** cylinder, **b** double cone, **c** truncated cylinder, and **d** double-truncated cone

and restrictions of the unit cell, could be of interest for estimating the effect of the particles for these materials.

4 Conclusions

In this study, the Halpin–Tsai model was modified for particulate-reinforced composites, using FEA estimations obtained for different particle geometries. There was found a new parameter (a), which depends on the angle of the particle corners, and could be introduced as a part of the shape-fitting parameter (ξ), modifying the Halpin–Tsai model. From the results obtained using this modified model, it can be concluded that the predicting ability of the Halpin–Tsai model could be improved, being possible to directly estimate the Young's modulus for different particle geometries by the introduction of the modified ξ. Predictions obtained using the modified Halpin–Tsai model were in better agreement with FEA estimations, and also with the experimental results, than the un-modified Halpin–Tsai estimations. Further, the results showed that Young's modulus and maxima stresses are highly dependent on the particle geometry, and the cylinder model presented the closest values to the experimental results and could be used for the estimation of the tensile properties of this kind of particulate-reinforced MMC, which present particles with a wide range of shapes.

Acknowledgments The authors would like to acknowledge the financial support from SENER–CONACYT 151496 and UNAM PAPIIT TA100114 for funding the project.

References

1. Engineered Materials Handbook. Volume 1: Composites (1989). ASM International, Metals Park, Ohio
2. Manna A, Bains HS, Mahapatra PB (2010) Experimental study on fabrication of Al–Al_2O_3/Grp metal matrix composites. J Compos Mater 45:2003–2010
3. Everett RK, Arsenault RJ (eds) (1991) Metal matrix composites: processing and interface. Academic Press, New York
4. Wilson S, Ball A (1990) Tribology of composite material. ASM International, Metals Park, Ohio
5. Rafiee M, He XQ, Mareishi S, Liew KM (2014) Modeling and stress analysis of smart CNTs/fiber/polymer multiscale composite plates. Int J Appl Mech 6(3):23
6. Hashin Z, Rosen BW (1964) The elastic moduli of fiber-reinforced materials. J Appl Mech 31(2):223–232. doi:10.1115/1.3629590
7. Feng S, Cui X, Li G (2014) Thermo-mechanical analyses of composite structures using face-based smoothed finite element method. Int J Appl Mech 6(2):17
8. Aghdam MM, Smith DJ, Pavier MJ (2000) Finite element micromechanical modelling of yield and collapse behaviour of metal matrix composites. J Mech Phys Solids 48:499–528
9. Halpin JC, Tsai SW (1967) Environmental factors in composite materials design. Air Force Materials Laboratory, TR 67-423
10. Wu Y, Jia Q, Sheng D, Zhang L (2004) Modeling Young's modulus of rubber–clay nanocomposites using composite theories. Polym Test 23(8):903–909
11. Cook RD, Malkus DS, Plesha ME (1989) Concepts and applications of finite element analysis, 3rd edn. Wiley, New York

12. Ganesh VV, Chawla N (2005) Effect of particle orientation anisotropy on the tensile behavior of metal matrix composites: experiments and microstructure-based simulation. Mater Sci Eng A 391:342–353
13. Kari S, Berger H, Gabbert U (2007) Numerical evaluation of effective material properties of randomly distributed short cylindrical fibre composites. Comput Mater Sci 39:198–204
14. Liu YJ, Chen XL (2003) Continuum models of carbon nanotube-based composites using the boundary element method. Electron J Boundary Elem 1:316–335
15. Pahlavanpour M, Moussaddy HH, Ghossein E, Hubert P, Levesque M (2013) Prediction of elastic properties in polymer–clay nanocomposites: analytical homogenization methods and 3D finite element modeling. Comput Mater Sci 79:206–215
16. Alfonso I, Figueroa IA, Sierra JM, Abatal M, Gonzalez G, Rodriguez-Iglesias V, Medina-Flores A, Flores JE (2013) Young's modulus estimation based on high symmetry 3-D finite element model for metal matrix composites. Comput Mater Sci 69:304–310
17. Karevan M, Pucha RV, Bhuiyan MdA, Kalaitzidoul K (2010) Effect of interphase modulus and nanofiller agglomeration on the tensile modulus of graphite nanoplatelets and carbon nanotube reinforced polypropylene nanocomposites. Carbon Lett 11:325–331
18. Huang Y, Jin KK, Ha SK (2008) Effects of fiber arrangement on mechanical behavior of unidirectional composites. J Compos Mater 42:1851–1871
19. Jung HK, Cheong YM, Ryu HJ, Hong SH (1999) Analysis of anisotropy in elastic constants of SiCp/2124 Al metal matrix composites. Scripta Mater 41:1261–1267
20. McLean A, Soda H, Xia Q, Pramanick AK, Ohno A, Motoyasu G, Shimizu T, Gedeon SA, North T (1997) SiC particulate-reinforced aluminium-matrix composite rods and wires produced by a new continuous casting route. Compos Part A 28:153–162
21. Gurrum SP, Zhao J, Edwards DR (2011) Inclusion interaction and effective material properties in a particle-filled composite material system. J Mater Sci 46(1):101–107. doi:10.1007/s10853-010-4844-2
22. Engineered Materials Handbook. Volume 2: Properties and Selection: Nonferrous Alloys and Special-Purpose Materials (1990) ASM International, Metals Park, Ohio
23. Chawla N, Shen Y (2001) Mechanical behavior of particle reinforced metal matrix composites. Adv Eng Mater 3:357–370
24. Chawla N, Chawla KK (2006) Microstructure-based modeling of the deformation behavior of particle reinforced metal matrix composites. J Mater Sci 41:913–925
25. Srivastava VK, Gabbert U (2011) Analysis of particles loaded fiber composites for the evaluation of effective material properties with the variation of shape and size. Int J Eng Sci Technol 3:52–68